The following publication X. Zhang, A. Bruce, S. Rowland, V. Terzija and S. Bu, "Modeling the development of low current arcs and arc resistance simulation," in IEEE Transactions on Dielectrics and Electrical Insulation, vol. 25, no. 6, pp. 2049-2057, Dec. 2018 is available at https://doi.org/10.1109/TDEI.2018.007100.

# Modelling the Development of Low Current Arcs and Arc Resistance Simulation

Xin Zhang, *member, IEEE*, Simon M. Rowland, *Fellow, IEEE*, Siqi Bu, *member, IEEE*, Jiebei Zhu, *member, IEEE*, and Vladimir J. Terzija, *Fellow, IEEE*

***Abstract*—Low current arcs in the range 0.5 mA~10 mA occur in power networks in situations such as on overhead line insulators and cable terminations. These are important because of their potential contribution to surface aging and asset failure. In this paper, the development of low current arcs is classified in three stages: the formative low current phase (~μA), a stage where discharges occur but are unstable with each half power cycle (<1 mA) and stable discharges (>1 mA). Arc resistance is a key element in controlling arc behavior in each stage, and is modelled as the combination of a stable arc resistance, an oscillating resistance and a surface resistance. The resulting arc model has been tested in PSCAD/EMTDC, to simulate an arc/discharge in each development stage. Simulations compare well with experimental data. The simulation reveals that peak arc current plays a key role in the transition from an unstable to stable arc. Arc energy analysis shows a significant energy increase as a result of arc stabilization. These models explain the conditions required for accelerated aging of polymeric insulators and can be used to design and interpret testing regimes, and understand the asset state for polymeric insulator management.**

***Index Terms*— Electrical discharge, arc, modelling, simulation, high voltage, polymeric insulators, laboratory test, arc resistance, energy, PSCAD, EMTDC, asset management, prognostics**

## I. Introduction

LOW amplitude surface currents and resulting discharges and arcs are a concern in polymeric outdoor insulation design and management. Components such as overhead line insulators, cable and transformer bushings, and all-dielectric, self-supporting (ADSS) cables are subject to electric fields and surface leakage currents. Resulting surface discharges and arcs [1-4] can lead to surface erosion and tracking, thereby reducing the reliability of insulation. This may eventually lead to mechanical failure of insulators, flashover or the puncture of bushings [5-9].

It has been established that the current and voltage supporting surface discharges is critical to the rate at which they cause surface damage. Previous simulation work on electrical arcs has been mainly based on high current flashover over long distances [10-11], or short arcs between high current contacts [12-13]. Modeling of low current arcs is less well developed and presently, low current arc models are applicable only to arc discharges in equilibrium [14-15]. No model has yet been proposed to simulate the dynamic development of the electrical properties of low current arcs.

Experimental work has identified two forms of discharge during low current arc development: unstable discharges with peak currents typically less than ~1 mA, and stable arcs with peak currents typically above ~1 mA. These are distinguished by whether a discharge is stable within half a power cycle. The transition between unstable discharges and stable arcs has been confirmed in laboratory conditions [16]. It has also been observed that the phase relationship between voltage and current changes as discharges and arcs appear. This typically occurs in a formative stage when a dry capacitive insulation surface is gradually replaced by resistive moisture, meaning voltage and current traces move from being 90 degrees out of phase to becoming in-phase. At this stage the leakage current grows until a value of typically to a level of ~0.6 mA, and then forms unstable discharges.

Based on experimental results [16], the three stages are here simulated in PSCAD/EMTDC: low current growth, unstable discharge and stable arc. Arc resistance is modelled as three sub-units named stable arc resistance, oscillating resistance and surface resistance. The discharge/arc voltage and current in the three stages are simulated, allowing associated arc energies to be analyzed. Simulation results are then compared with experimental arc data indicating a good correlation. The proposed model is not only capable of modelling low current discharge/arc behavior, but also able to simulate arc voltage and current features in each development stage.

## II. Laboratory Test and Results

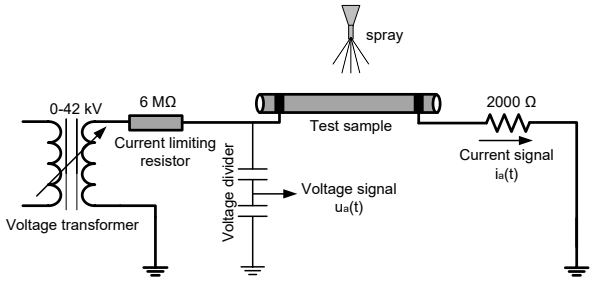


Fig. 1. The experimental setup

Detailed test procedures have been reported previously [16]. The experimental set up is summarised in Fig. 1. A silicone sheathed pultruded rod of outer diameter 22 mm is tested with

Xin Zhang and Jiebei Zhu are with National Grid, Wokingham, RG41 5BN, United Kingdom, (e-mail: xin.zhang@nationalgrid.com)

Simon. M. Rowland and Vladimir. J. Terzija are with the University of Manchester, Manchester, M60 1QD, United Kingdom.

Siqi Bu is with Hong Kong Polytechnic University, Kowloon, Hong Kong.

electrodes directly attached and separated by 200 mm. Water of conductivity 16,000 µS/cm is sprayed in the surface and a variable voltage of 0 to 42 kV (peak) applied. The data acquisition system (PC and labview) include a voltage divider with the ratio of 1:10,000 to obtain the voltage at the HV end of the rod (approximately the discharge voltage), and a 2000 Ω resistor (R2) to enable measurement of the leakage current.

### A. *Formative Low Current Phase*

In the early stage of moisture deposition on the sample surface, the voltage and current traces are initially 90 degrees out of phase (capacitive), and gradually become in phase (resistive), as shown in Fig. 2. The leakage current increases due to the continuous moisture formation on the silicone surface, which reduces the surface resistance. No arcing activities are observed at this stage.

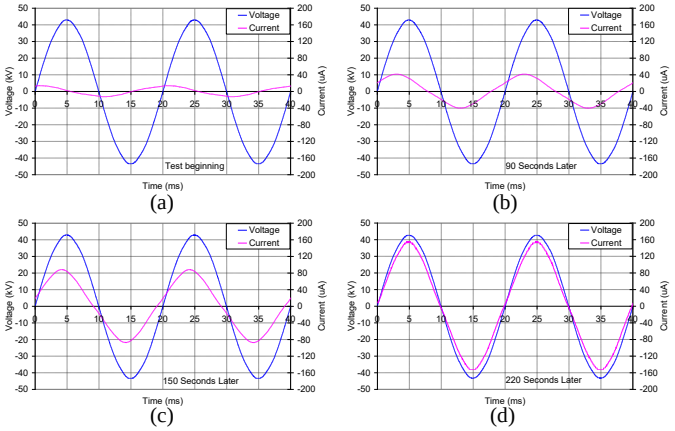


Fig. 2. Voltage and current curves show, as the current increases: (a) time 0, voltage lags current by 90 degrees; (b) at 90 seconds from test start, voltage lags current by 60 degrees; (c) at 150 seconds from test start, voltage lags current by 30 degrees; (d) at 220 seconds, voltage and current are in phase.

### B. *Unstable Discharges*

Unstable discharges are observed for currents over 0.6 mA. In these cases the applied voltage is high enough to strike an arc across a dry band on the insulator, but the current is insufficient to sustain an arc, so that the discharge is 'unstable'. Following the discharge development, typically after an extended 2 minutes of wetting time, the peak discharge current gradually increases. This could due to the increase in surface conductivity of the insulator, or a reduction in the natural discharge length [16-17]. Increased peak current is accompanied by discharges gradually become stable arcs, with less oscillation of arcing voltage and current, as seen in Fig. 3. The development time from an unstable discharge to a stable arc varies dependent on the spray rate. In this test, a spray rate of 0.12 g/cm$^2$/hr is used throughout the test. It is observed that higher spray rate would accelerate the arc development process, due to the more effective moisture deposition on insulation surface.

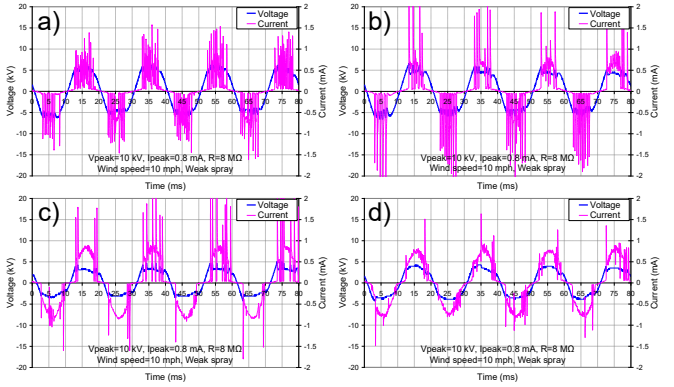


Fig. 3. Unstable discharges become more stable arcs: (a) Initial unstable discharges appear after 10 minutes from test start, (b) Reduced instability and discharge oscillation frequency after 12 minutes, (c) Stable arcs appear but are accompanied by some instability after 15 minutes, (d) Stable arcs finally dominate after 20 minutes.

### C. *Stable Arcs*

When equilibrium is achieved between an electrical arc and surrounded moisture conditions, stable arcs appear with smooth and repeatable voltage and current characteristics, typically when the arc current is above 1.0 mA. In Fig. 4, the impact of increasing the source voltage to generate 1.5 mA, 2.0 mA, 2.5 mA, 3.0 mA, 3.5 mA and 4.0 mA arcs is shown. Each test is conducted for at least 30 minutes to allow equilibrium to be established. These current and voltage traces are of the classical 'dry-band arc' form, but of lower current magnitude than is normally studied.

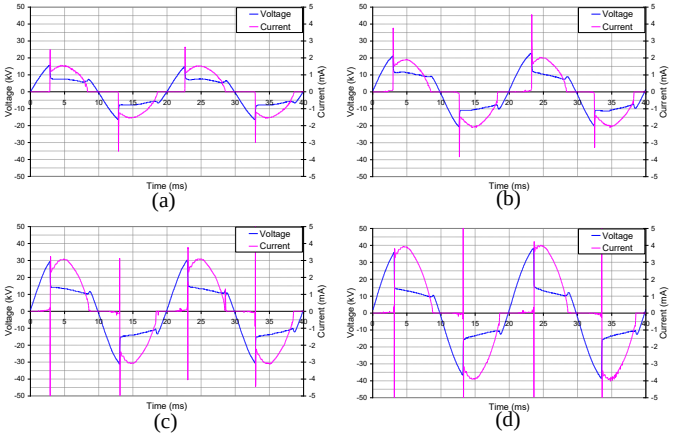


Fig. 4. Voltage and current curves show stable arcs with: (a) 1.5 mA; (b) 2.0 mA; (c) 3.0 mA; (d) 4.0 mA.

## III. Arc Resistance Modelling

The stability of an arc is determined by two things. Firstly sufficient voltage is required to strike an arc across a high resistance gap. Secondly, once the arc is established, it can only be maintained if sufficient voltage remains available across the lower resistance arc to maintain the current flow. The available voltage is dependent on the supply voltage and ratio of the resistance of the arc to the resistance of the supply circuit (which is normally the resistance of the rest of the insulator surface, but in this case is that of the ballast resistor). In turn,

the resistance of the arc is a strong function of current, which is controlled by the supply circuit which in this situation has a higher resistance than the arc itself. Arc resistance is a thus a key parameter in the arc development process.

In this paper, arc resistance is simulated in the in PSCAD/EMTDC software package as 'Stable Arc Resistance' in series with 'Oscillating Resistance', and 'Surface Resistance', as shown in Fig. 5. Stable arc resistance represents the well-established stable arc characteristic, oscillating resistance simulates unstable discharge characteristics, and the surface resistance is used to simulate the low current pre-discharge stage.

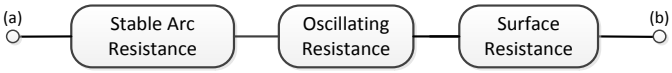


Fig. 5. The simulation of arc resistance consists of 'stable arc resistance', 'oscillating resistance' and 'surface resistance' for different stages in arc development.

### A. *Stable Arc Resistance*

For stable arcs, three periods are identified within each half cycle in Fig. 6 as pre-arcing, arcing and post-arcing periods. A detailed mathematical model to simulate voltage and current traces for each period are reported and validated elsewhere [17]. In this paper, the accuracy of that model is improved by simulating arcing voltage $u_a(t)$ with a sloping line from $U_{t1}$ (arc ignition voltage) to $U_{t2}$ (arc extinction voltage). The model is also extended to simulate arcs for different current levels, $I_a$ (peak current). The new model gives between times $t_1$ and $t_2$,

$$u_a(t) = U_{t1} - \frac{U_{t1} - U_{t2}}{t_2 - t_1}(t - t_1) \tag{1}$$

$$i_a(t) = \sqrt{2} I_a \sin \omega_i [t - (\frac{\pi}{\omega_u} - t_2)] \tag{2}$$

where: $I_a$ and $\omega_i$ are the rms value (mA) and angular frequency (rad/ms) of the sinusoidal current, $U_a$ and $\omega_u$ are the rms value (mA) and angular frequency (rad/ms) of the source voltage, $t_1$ is the arc ignition time (ms), $t_2$ is the arc extinction time (ms), $U_{t1}$ is the arc ignition voltage (kV), and $U_{t2}$ is the arc extinction voltage (kV).

The stable arc resistance between times $t_1 < t < t_2$ is then given by

$$r_a(t) = \frac{u_a(t)}{i_a(t)} = \frac{U_{t1} - \frac{U_{t1} - U_{t2}}{t_2 - t_1}(t - t_1)}{\sqrt{2} I_a \sin \omega_i [t - (\frac{\pi}{\omega_u} - t_2)]} = \frac{dt + e}{a \sin(bt + c)} \tag{3}$$

Arc length is reported as an important parameter for arc resistance [10]. The relevant experimental data is summarized in Table I. Arc peak current ($I_a$), arc ignition voltage ($U_{t1}$), and arc extinction voltage ($U_{t2}$) are linked to arc length ($L_a$) by the fitting method of least square estimator (LSE). Substituting $U_{t1}$, $U_{t2}$, $t_1$, $t_2$, the stable arc resistance for an arc of length $L_a$ is given by,

$$r_a(t, L_a) = \frac{1.2L_a + 5.65}{(0.45L_a + 0.70)\sin 0.427(t - 1.32)} \tag{4}$$

where 2.98 ms < t < 8.68ms;

TABLE I
Summary of Test data in Low Current Stable Arcs

| Arc Length ($L_a$ cm) | Arcing Current (Ia mA) | $U_{t1}$ kV | $U_{t2}$ kV | $t_1$ ms | $t_2$ ms |
|---|---|---|---|---|---|
| 1.83 | 1.5 | 7.91 | 6.54 | 2.84 | 8.73 |
| 2.82 | 2 | 11.33 | 8.3 | 2.87 | 8.42 |
| 3.81 | 2.5 | 11.13 | 8.01 | 2.61 | 8.76 |
| 5.27 | 3 | 14.75 | 10.64 | 3.01 | 8.68 |
| 6.37 | 3.5 | 16.8 | 11.91 | 3.13 | 8.66 |
| 7.07 | 4 | 15.04 | 10.64 | 3.43 | 8.84 |
| **$L_a$** | **$0.45L_a+0.70$** | **$1.49L_a+6.09$** | **$0.91L_a+5.20$** | **2.98** | **8.68** |

The arc resistance for a given arc length can be calculated from (4), and is shown to be a good fit to the corresponding measured arcs in Fig. 7.

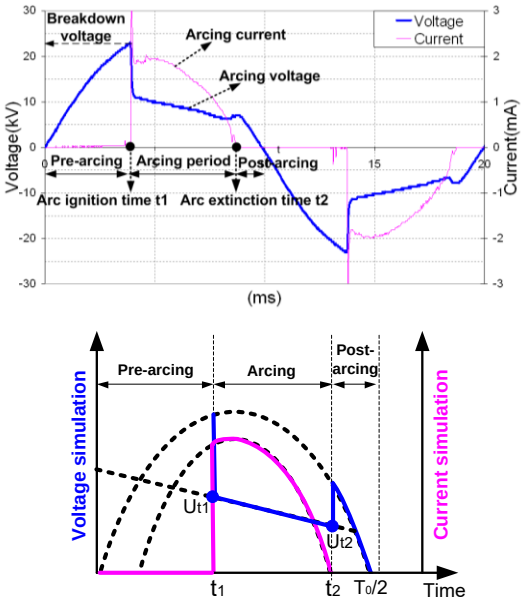


Fig. 6. Double sinusoidal model to simulate I-V curves for stable arcs. The upper curve is from experiments illustrating the whole power cycle. The lower image shows the sinusoidal model.

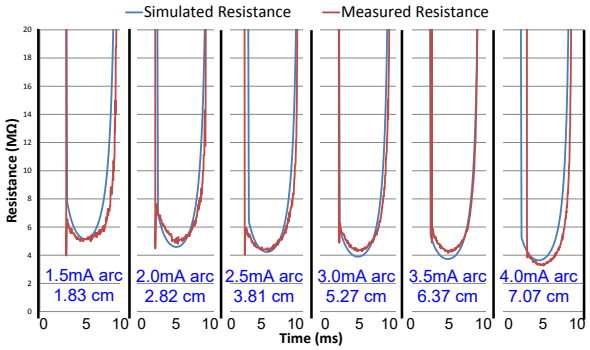


Fig. 7. Simulated and measured arc resistances for current levels from 1.5mA to 4.0mA through complete half cycles.

### B. *Unstable Discharge Resistance*

Unstable discharges repeatedly switch the arc on and off due to insufficient current being available to sustain an arc. This phenomenon is modelled as a rapid increase in discharge resistance when an arc is switched off. Equation (5) proposes an 'oscillating resistance' that generates impulses at frequency f, impulse width of Ɛ and peak value of $R_Ɛ$, as shown in Fig. 8.

$$r_{oscillating} = R_v\left\{sign[\sin(2\pi ft)] - sign[\sin 2\pi f(t-\varepsilon)]\right\} \quad (5)$$

By observing the oscillating features of unstable discharges from test results, each oscillation period takes approximate 0.01 ms, so the impulse width Ɛ is set to 0.01 ms. The impulse peak $R_Ɛ$ requires a high value to switch off the discharge. In this case $R_Ɛ$ is chosen at 50 MΩ, which is 10 times higher than the measured stable arc resistance. Impulse frequency f starts from approximate 2000 Hz for 0.6 mA unstable discharge, and reduces to 0 Hz for a 1.0 mA stable arc.

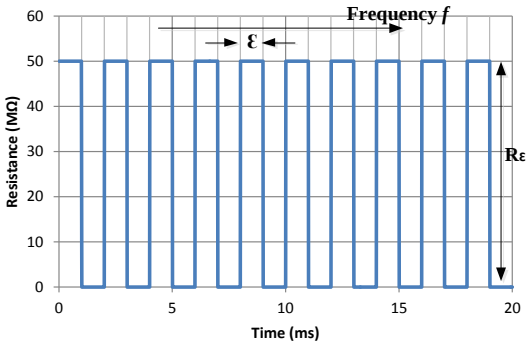


Fig. 8. The modelling of oscillating resistance with frequency f, impulse width Ɛ, and impulse peak $R_v$.

The oscillation frequency f is a function of discharge peak current $I_a$ and the model adopted is proposed in (6). Experimental results in Fig. 2 show that when the discharge current peak $I_a$ increases from 0.6 mA to 1.0 mA, the vibration frequency f drops from 2000 Hz to 0 Hz representing a more stable discharge. A linear relationship is assumed between f and $I_a$ for 0.6 mA < $I_a$ < 1.0 mA so that

$$f = -2500I_a + 2500 \quad (6)$$

The resulting resistance, based on (5) and (6), is shown in Fig. 9 a). The entire unstable discharge resistance is modelled in PSCAD/EMTDC as the stable arc resistance (with current < 1mA) in series with the oscillating resistance as shown in Fig. 9 b).

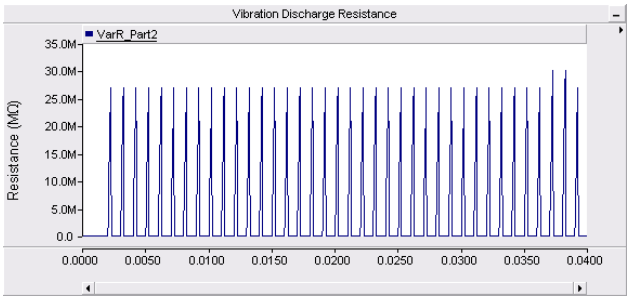


(a) The vibration unit to simulate unstable discharges at 1000Hz

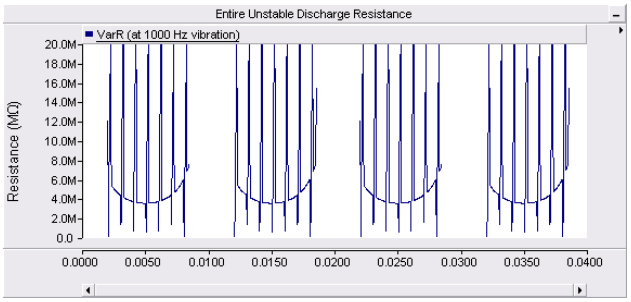


(b) Entire unstable discharge resistance with combination of vibration resistance and stable arc resistance

Fig. 9. (a) The vibration resistance to simulate unstable discharges at 1000Hz, (b) Entire unstable discharge resistance with combination of oscillating resistance and stable arc resistance.

### C. *Surface Resistance*

Before arc discharges appear, the material surface is modelled as a variable resistance in parallel with a capacitor as shown in Fig. 10. When the sample surface is still dry, the variable resistor taps at point 'a' with an extremely high value (~200 MΩ). The majority of leakage current is flowing in the capacitor path given an initial dry current of 14 μA corresponding to the capacitance calculated around 1 pF. The current leads the voltage at this stage.

When the sample becomes wet due to the moisture deposition, the value of dry resistance drops, to the value of ~10 Ω (equivalent to a moisture conductivity of 16,000 μs/cm), which will shunt the capacitor and make surface effectively resistive, and the current flows in phase with the voltage.

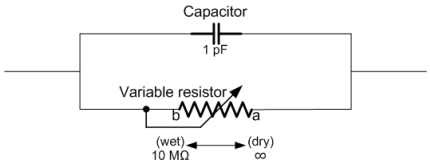


Fig. 10. Electrical model of silicone rubber sample surface in dry and wet conditions.

The simulated surface impedance is,

$$Z_{surface} = \frac{\frac{R_{var}}{\omega C}}{R_{var} + \frac{1}{\omega C}} \quad (7)$$

where $R_{var}$ is variable resistance from 200 MΩ to 10 Ω, ω is angular frequency at 50Hz, C is fixed at 1pF.

## IV. ARC SIMULATION IN PSCAD/EMTDC

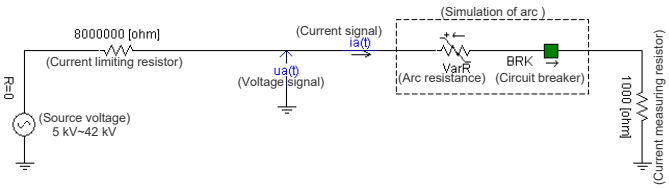


Fig. 11. Simulation circuit of low current arc discharge in PSCAD

The PSCAD simulation was built as shown in Fig. 11. The source voltage is produced by an a.c 50 Hz generator (output range 5-42 kV), with a current limiting resistor of 8 MΩ.

The simulation of arc resistance consists of three blocks in PSCAD: stable arc resistance, oscillating resistance and surface resistance, as shown in Fig. 12. The stable arc resistance block is constructed based on (4), oscillating resistance block is based on (5-6), and surface resistance block is based on (7). The coordination function between three blocks is given in table II.

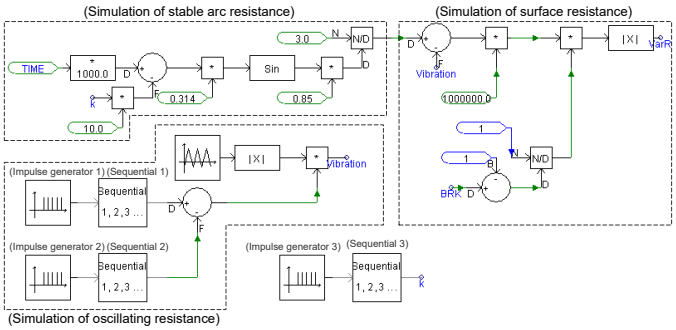


Fig. 12. Simulation circuit for arc resistance consists of stable arc resistance, oscillating resistance, and surface resistance.

TABLE II
The coordination between Stable Arc Resistance, Vibration Resistance and Surface Resistance

| Stage | Arc Current (mA) | Stable Arc Resistance | Oscillation Resistance | Surface Resistance |
|---|---|---|---|---|
| Phase Shifting | <0.6 | 0 | 0 | Equation (7) |
| Unstable Discharge | 0.6 – 1.0 | Equation (4) | Equations (5,6) | 0 |
| Stable Arc | 1.0 – 5.0 | Equation (4) | 0 | 0 |

The control signal BRK operates the circuit breaker to simulate arc discharge ignition and extinction at times $t_1$ and $t_2$. The BRK control circuit is shown in Fig. 13. Impulse Generator 1 was set to 100 Hz with a first impulse at $t_1$ (arc ignition time). Impulse Generator 2 was also set to 100 Hz with a first impulse at $t_2$ (arc extinction time). These two impulse generators coordinate with two Sequential Units to generate the 'BRK' control signal shown in Fig. 14. From $t_1$ (2.98ms) to $t_2$ (8.68ms), 'BRK' brings the arc resistance into the circuit.

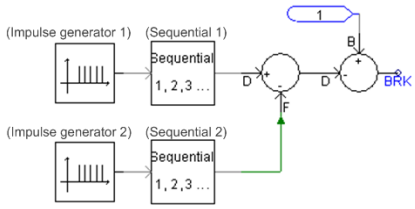


Fig. 13. Simulation circuit to produce a control signal 'BRK'

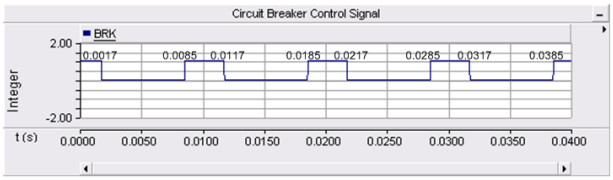


Fig. 14. The output of control signal BRK for arc ignition and extinction

### A. *Simulation of Unstable Discharges*

The simulation results for unstable discharges and the transition process from unstable to stable conditions are shown in Fig. 15. The correlation coefficients are above 0.75 for all cases between the simulation and experiment results. The PSCAD simulation here reflects the main electrical features of unstable discharges. It can also simulate the reduced oscillation frequency when arc peak current rises from 0.6 mA to 1.0 mA. This is a key development feature from unstable discharges to stable low current arcs.

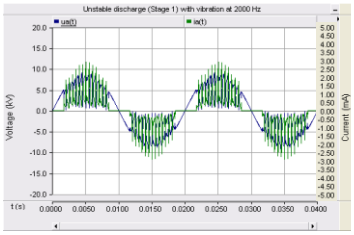

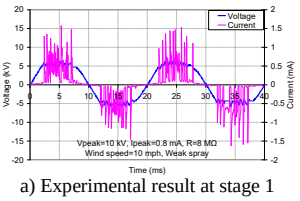


a) Experimental result at stage 1

(a) Unstable discharges (0.6mA) with oscillation frequency at 2000 Hz

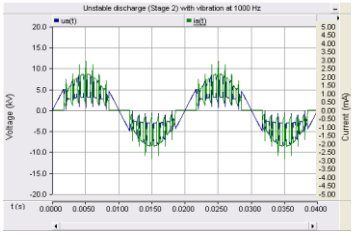

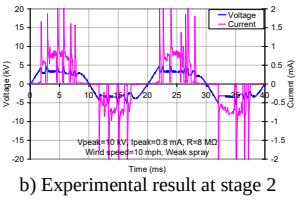


b) Experimental result at stage 2

(b) Unstable discharges (0.8mA) with an oscillation frequency of 500 Hz

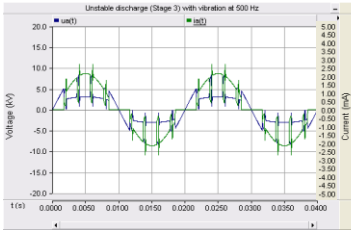

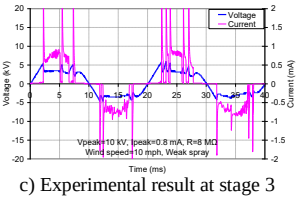


c) Experimental result at stage 3

(c) Nearly stable arc (0.9mA) with an oscillation frequency of 250 Hz

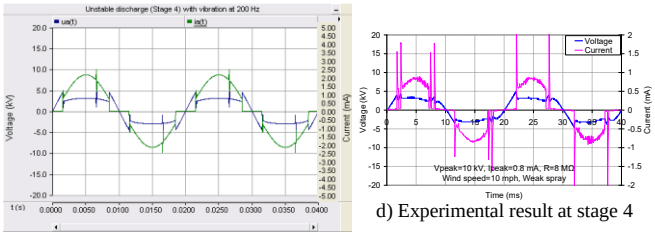


d) Experimental result at stage 4

(d) Mainly stable arcs (0.95mA) dominate with oscillation at around 100 Hz

Fig. 15. Simulation result for unstable discharges as current increases.

### *B. Simulation of Stable Arcs*

By running the PSCAD simulation for stable arcs, the voltage and current curves for arcs with respectively 1.5 mA, 2.0 mA, 3.0 mA and 4.0 mA peak current can be obtained in Fig. 16. Correlation coefficients above 0.95 confirm the validity of the PSCAD simulation for simulating stable arcs.

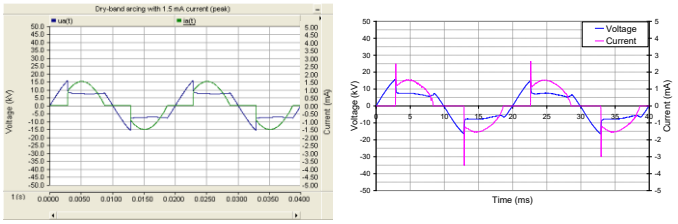


(a) Simulated stable arc of 1.5 mA (left) compared with experiment (right)

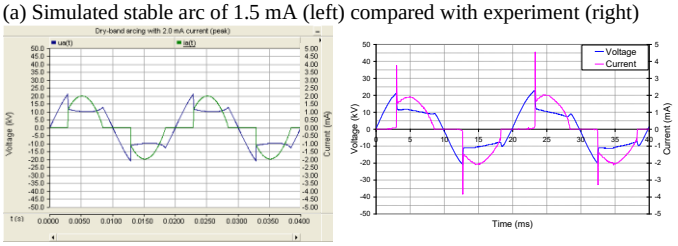


(b) Simulated stable arc of 2.0 mA (left) compared with experiment (right)

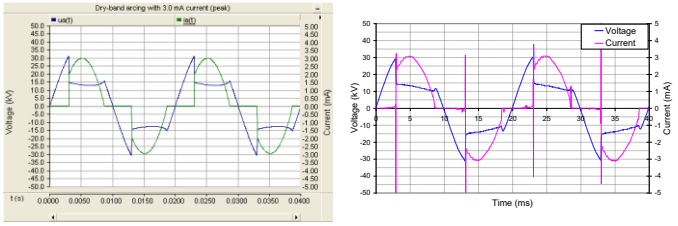


(c) Simulated stable arc of 3.0 mA (left) compared with experiment (right)

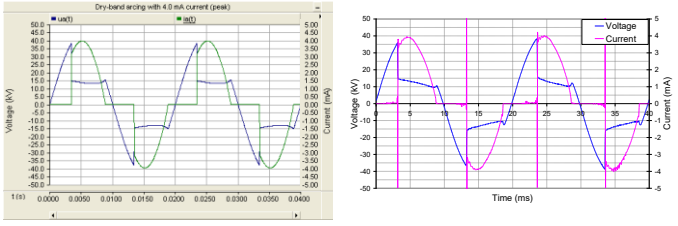


(d) Simulated stable arc of 4.0 mA (left) compared with experiment (right)

Fig. 16. Simulation of stable arcs at different current levels from 1.5 mA to 4.0 mA.

## V. Discussion

The stability of low current discharges has been previously explored using experimental methods [16]. The low current arc behaves an oscillating feature in voltage and current for a range of 0.6 mA to 1.0 mA. The modelling of unstable discharges here reveals a relationship between oscillation frequency f and discharge peak current $I_a$. Equation (8) also quantifies this relationship. When the discharge peak current increases from 0.6 mA to 0.95 mA, the oscillation frequency reduces from 2000 Hz to 100 Hz, representing a more stable arc.

The transition from unstable discharges to stable arcs is a critical process that increases arc energy and so presents an increased threat to the surface of polymeric insulation. Previous experiment work reveals that the measured changes in arc energy are up to 3 times from an initial unstable state to a well-developed stable state [16,17]. Based on the simulated arc voltage and current from PSCAD, the arc energy per half a cycle is calculated as:

$$E_a = 2\int_0^{\pi} u_a(t) i_a(t) dt \tag{8}$$

where: $E_a$ is arc energy (Joule) per cycle, $i_a(t)$ is the simulated arc current curve, and $u_a(t)$ is the simulated voltage curve.

The energy trend as the discharge activity transitions from unstable discharges to stable arcs is shown in Fig.17 for both PSCAD simulation and experiment results. Increased arc energy has been found in the development process from unstable discharges to stable arcs. This is due to the increase in discharge current and reduction in oscillation which prolongs the total arcing period per power cycle. In addition, 0.01 Joule / cycle is identified as a threshold to distinguish between unstable discharges and stable arc.

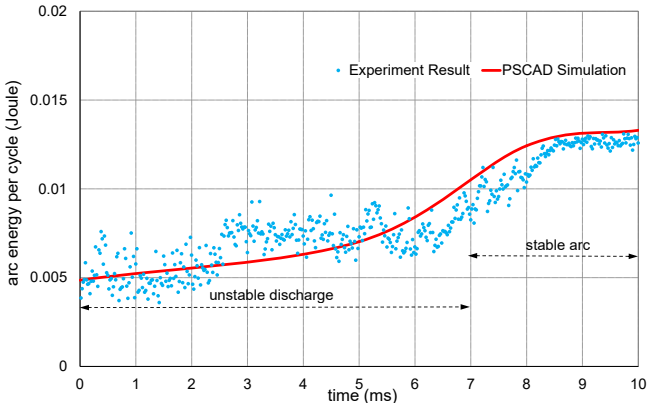


Fig. 17. Arc energy trends from unstable discharges to stable arcs for both PSCAD simulation and experiment results

The modelling approach here allows a deeper understanding of energy change during the discharge/arc transition process, and provides a tool by which the energy in a discharge can be calculated and monitored. This may be developed into an online monitoring system that measures real discharge current and converts into arc energy through the designed PSCAD simulation program.

## VI. Conclusion

The development of low current arc discharges between 10 μA and 5 mA has been classified into three stages: pre-discharge current, unstable discharge and stable arcs. Arc resistance is modelled in three states: surface resistance, oscillating resistance and stable resistance. Equations which describe each resistance stage have been developed, together with a control logic to coordinate the respective regimes. A circuit was built in PSCAD to simulate the arc voltage and current in corresponding development stages. It has been found that the experimentally observed increase of discharge stability with peak current, at around 1 mA, is reproduced well in the model. Similarly an increase in thermal energy is reproduced in the model. The change in arc stability so characterized, provides an indication of enhance power in the arc and so identifies situations in which more aggressive/accelerated ageing of a polymer surface may occur.

## VII. References


[1] R. S. Gorur, E. A. Cherney and J. T. Burnham, Outdoor Insulators, ISBN 0-9677611-0-7, Phoenix, Arizona, USA, 1999.

[2] C. N. Carter, "Dry Band Electrical Activity on Optical Cables Strung on Overhead Power Lines," in Proc. 37th International Wire and Cable Symposium, 1988, pp. 117-121.

[3] S. M. Rowland, "Prevention of dry-band arc damage on ADSS cables," IEEE Trans. Dielectrics and Electrical Insulation, vol. 13, pp. 765-772, 2006.

[4] Z. Jia, C. Chen, X. Wang and H. Lu, "Leakage Current Analysis on RTV Coated Porcelain Insulators During Long Term Fog Experiments," IEEE Trans. Dielectrics and Electrical Insulation, vol. 21, pp. 1547-1553, 2014.

[5] S. M. Rowland, K. Kopsidas and X. Zhang, "Ageing of Polyethylene ADSS Sheath By Low Currents" IEEE Trans. Power Delivery vol. 25, pp. 947-952, 2010

[6] Y. Xiong, S. M. Rowland, J. Robertson and R. J. Day, "Surface Analysis of Asymmetrically Aged 400 kV Silicone Rubber Composite Insulators", IEEE Trans. on Dielectrics and Electrical Insulation, Vol. 15, pp. 763-770, 2008.

[7] S. E. Kim, E. A. Chemey and R. Hackam, "Effect of Dry Band Arcing on the Surface of RTV Silicone Rubber Coatings", IEEE Int. Symp. on Electrical Insulation Baltimore, MD USA, pp. 237-240, 1992.

[8] Y. Zhu, M. Otsubo, N. Anami, C. Honda, O. Takenouchi, Y. Hashimoto, and A. Ohono, "Change of Polymeric Material Exposed to Dry Band Arc Discharge [Polymer Insulator Applications]", Conference on Electrical Insulation and Dielectric Phenomena, 2004, pp. 655-658.

[9] M. Kumosa, L. Kumosa and D. Armentrout, "Failure Analyses of Nonceramic Insulators Part 1: Brittle Fracture Characteristics", IEEE Electrical Insulation Magazine. Vol. 21, May/June, pp. 14-27, 2005.

[10] V. V. Terzija and H. J. Koglin, "On the modeling of long arc in still air and arc resistance calculation," IEEE Trans. on Power Delivery, vol. 19, pp. 1012-1017, 2004.

[11] V. V. Terzija, G. Rreston, M. Popov and N. Terzija, "New Static 'AirArc' EMTP Model of Long Arc in Free Air," IEEE Transactions on Power Delivery, vol. 26, pp. 1344-1353, 2011.

[12] P. Borkowski and E. Walczuk, "Thermal models of short arc between high current contacts," in Proceedings of the Forty-Seventh IEEE Holm Conference on Electrical Contacts, 2001, pp. 259-264.

[13] S. Nitu, C. Nitu, and P. Anghelita, "Electric Arc Model, for High Power Interrupters," in The International Conference on Computer as a Tool, Eurocon, pp. 1442-1445, 2005

[14] Q. Huang, G. G. Karady, B. Shi and M. Tuominen, " Numerical Simulation of Dry-band Arcing on the Surface of ADSS Fiber-optic Cable," IEEE Trans. Dielectrics and Electrical Insulation, vol. 12, No. 3, pp. 496-503, 2005.

[15] X. Zhang and S. M. Rowland, "Modelling of dry-band discharge events on insulation surfaces," 2010 IEEE International Symposium on Electrical Insulation (ISEI), San Diego, California, USA, pp. 1-5, 2010.

[16] X. Zhang and S. M. Rowland, " The Stability and Energy of Low Current Surface Discharges on Wet Surfaces," IEEE Trans. Dielectrics and Electrical Insulation, vol. 19, Issue 6, pp. 2055-2062, 2012.

[17] X. Zhang, S. M. Rowland, and V. Terzija, "Increased energy in stable dry-band arcs due to length compression," IEEE Transactions on Dielectrics and Electrical Insulation, vol. 17, pp. 473-480, 2010.


**Xin Zhang** (M'17) was born in Shandong, China. He received the B.Eng. degree in automation from Shandong University, China, in 2007, the M.Sc. and Ph.D. degrees in electrical poewr engineering from The Univerisity of Manchester, United Kingdom, in 2007 and 2010 respectively.

He currently works as a Power System Engineer at National Grid, Wokingham, United Kingdom. His research interests include high voltage engineering, and power system planning, operation, and control.

Dr. Zhang is a Chartered Engineer wih UK Engineering Council.

**Prof Simon M Rowland** (F'14) was born in London, England. He completed the B.Sc. degree in physics at The University of East Anglia, and the PhD degree at London University, UK.

He has worked for many years on dielectrics and their applications and has also been Technical Director within multinational companies. He joined The School of Electrical and Electronic Engineering in The University of Manchester in 2003, and was appointed Professor of Electrical Materials in 2009, and Head of School in 2015.

Prof. Rowland was President of the IEEE Dielectric and Electrical Insulation Society in 2011and 2012.

**Siqi Bu** (S'11, M'12) received the Ph.D. degree from the electric power and energy research cluster, the Queen's University of Belfast, Belfast, U.K., in 2012, where he continued his postdoctoral research work before entering industry.

He joined National Grid UK as a Power System Engineer, and then became an experienced UK National Transmission System Planner and Operator. He has received various prizes due to excellent performances and outstanding contributions in operational and commissioning projects. He is an Assistant Professor with Hong Kong Polytechnic University and also a Chartered Engineer with UK Engineering Council. His research interests are power system stability analysis and operation control, including wind power generation, PEV, HVDC, FACTS and ESS.

**Jiebei Zhu** ( ) received the B.S. degree in microelectronics from Nankai University, Tianjin, China, and the M.Sc. and Ph.D. degrees in electronic and electrical engineering from the University of Strathclyde, Glasgow, U.K., in 2008, 2009 and 2013 respectively.

He is currently a Chartered Engineer with National Grid UK. His research interests involves with high voltage technologies including HVDC transmission system devices and control systems, renewable power generation and energy storage technologies.

**Vladimir Terzija** (M'95, SM'00, F'16) was born in Donji Baraci (former Yugoslavia). He received the Dipl-Ing., M.Sc., and Ph.D. degrees in electrical engineering from the University of Belgrade, Belgrade, Serbia, in 1988, 1993, and 1997, respectively.

He is the Engineering and Physical Science Research Council Chair Professor in Power System Engineering with the School of Electrical and Electronic Engineering, The University of Manchester, Man-chester, U.K., where he has been since 2006. From 1997 to 1999, he was an Assistant Professor at the University of Belgrade, Belgrade, Serbia. From 2000 to 2006, he was a Senior Specialist for switchgear and distribution automation with ABB AG Inc., Ratingen, Germany. His current research interests include smart grid application of intelligent methods to power system monitoring, control, and protection; wide-area monitoring, protection, and control; switchgear and fast transient processes; and digital signal processing applications in power systems.

Prof. Terzija is Editor in Chief of the International Journal of Electrical Power and Energy Systems, an Alexander von Humboldt Fellow, as well as a DAAD and Taishan Scholar.